

---

# Development of Experimental Apparatus for Metal Cutting Tests

Duarte M. F. Andrade  
duarte.andrade@ist.utl.pt

Instituto Superior Técnico, Universidade de Lisboa, Portugal  
June 2019

## Abstract

The present dissertation will address the development of an experimental apparatus to perform metal cutting tests under controlled laboratory conditions. This apparatus allows the control of cert test parameters, such as cutting speed, with high stability and rigidity. The tests were performed with and without addition of a lubricant in static and dynamic regime. The test specimens were manufactured in AA1050 aluminum. The influence of the lubrication will be evaluated through the morphological observation of the metal chip and the surface, as well as through the monitoring of the cutting forces. The results showed the influence of some parameters on the metal cutting tests, both at process and experimental development level, seeking to contribute to a better understanding of metal cutting processes.

**Keywords:** Metal cutting, experimental development, lubricant, cutting forces.

## 1. Introduction

Metal cutting is one of the most important manufacturing processes nowadays. In the automotive, aeronautical and electrical industries there are numerous machining tools, workshops and laboratories that employ tens of millions of workers around the world. The metal cutting process addresses the cutting of a thin layer from a softer metallic workpiece by the action of a harder tool in order to produce a chip. Chip formation occurs in a very small volume of metal, around the cutting edge, and determines the machinability of the material, the performance of the tools and the qualities of the machined surface.

Over time, metal cutting has been the object of a high theoretical and experimental study through scientific contributions. Numerous efforts have been made to describe this mechanism of chip formation, aiming at a clearer general understanding of the most

influential parameters in the process. Recently, the finite element methodology replaced the analytic models postulated by Lee and Shaffer (1951) and Merchant (1944) and managed to study the process more precisely. However, experimental work has become more consistent over time using more modern and robust equipment, as well as technologically more advanced data acquisition and instrumentation systems.

However, despite these developments, these contributions continue to show evidence that none of the attempts to achieve a chip trimming solution can represent the experimental data for a wide range of materials under different operating conditions, indicating that other phenomena related to the formation of the new surface must be considered.

In order to perform metal cutting experiments, test machines were developed throughout the years on IST's Manufacturing

and Process Technology facilities. Performing cutting tests requires an experimental apparatus, consisting in a test machine and a set of instrumentation and acquisition components, which will transmit the ongoing test data to a computer.

So far, all the experimental contributions in the orthogonal metal cutting were related to steady and quasi-steady state of velocity. It was through Fernandes (2017) that the first experimental apparatus for high velocity cutting test was developed, enabling cutting velocities of 200 m / min, value used by the author in some cutting tests (Figure 3).



Figure 3. Test machine developed by Fernandes (2017) for high speed metal cutting tests.

## 1.1. Metal Cutting

To study the behavior of materials subjected to metal cutting tests it's necessary to assume that the cutting process can be analyzed in a two-dimensional way, eliminating several variables of the process, making it more suitable for fundamental research analysis. This definition is termed orthogonal cutting, in which the tool's cutting edge is perpendicular to the cutting direction (Merchant, 1944).

The depth of the layer of material removed by the action of the tool is known as the undeformed chip thickness,  $e$ , and the chip thickness,  $e'$ , is the resulting of the shear on the shear plane, with an angle  $\phi$  to the direction of the cutting. These two thicknesses can be related through the chip compression ratio,  $R_c$ :

$$R_c = \frac{e'}{e} = \cot\phi \cos\alpha + \sin\alpha \quad (1)$$

The parameter used to obtain the efficiency of the process is the specific cutting pressure,  $k_s$ , given by the ratio between the cutting force  $F_c$  and the cross-sectional area of the undeformed chip  $A_0$ , expressed in MPa:

$$k_s = \frac{F_c}{A_0} \quad (2)$$

## 1.2. Tribology

The surfaces of solids play many different and important roles in technology. When clean metals rub against one another, adhesion can occur, raising the friction and promoting the deformation and fracture of the softer material. This friction takes an important role in the engineering functions; therefore, it must be measured and controlled.

Lubrication can be defined as the reduction of friction between two surfaces by reducing the level of interaction between the roughness (Myers, 1999). Placing a lubricant between two surfaces often dramatically lowers the friction coefficient. In such cases, the friction coefficient of the system is a function of the combined properties of the fluid and material surfaces. If the sliding members are fully separated by a film of lubricant, the friction coefficient of the system is essentially the friction coefficient of the fluid.

The classical approximation is based on Coulomb friction law (formulated in 1875) where the friction coefficient,  $\mu$ , is given by the relation between the force exerted by friction,  $F_f$ , and the force normal to the contact surface,  $F_N$ , and its expressed as:

$$\mu = \frac{F_f}{F_N} \quad (3)$$

## 2. Development of Experimental Apparatus

### 2.1. Test Machine

In order to perform the metal cutting tests, a test machine was developed by the author with the main purpose of guaranteeing a

elevated stiffness on the assembled parts so it can perform tests in a wider range of materials (Figure 4).

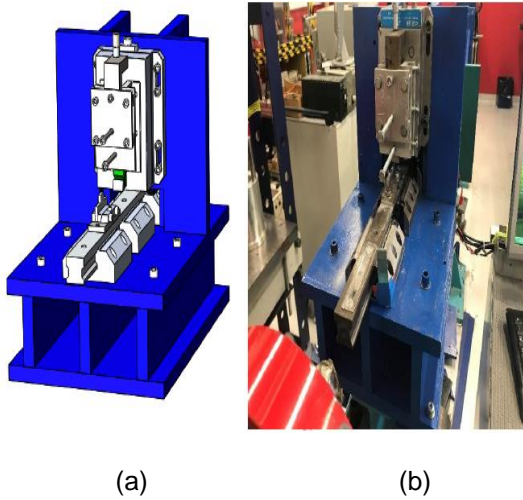


Figure 4. a) CAD project; b) Testing machine.

This test machine consists in a set of 8 large machined steel plates assembled together. To ensure great stiffness, close to 40 bolted connections were applied on this structure. In addition, 4 smaller plates were also dimensioned, designed to "fasten" the test machine to the supporting frame. The specimen's displacement into the cutting tool is guaranteed by a movable steel guide aligned by three bearing housings, as shown in the figure 4.

## 2.2. Load

### Load Cell

To measure the forces involved in the metal cutting process, the piezoelectric load cell Kistler® 9257A was selected (Figure 5). A piezoelectric sensor measures changes in pressure, acceleration or force, converting them into an electrical charge. This load cell was chosen based on its functionality and geometry, easily fitting into the main vertical plate that supports not only this cell but also the tool securing device.



Figure 5. Kistler® 9257A load cell.

## 2.3. Displacement

### Sensors

The inductive displacement sensors, based on magnetic induction, have the advantage that they do not require physical contact, potentially promoting wearing between these components, and are less sensitive to noise interferences. The selected sensors for this study are a set of two coils represented in figure 6, one as an inductor and another as a receiver, which when current flows in the inductor coil it produces a variable magnetic field, stimulating the receiver coil, depending on the distance between them.



Figure 6. a) Inductor moving coil; b) Steady receiver coil.

### Rectifier

The data acquisition board only reads DC signals and given this impedance, it was necessary to create a current rectifier to convert the signal from AC to DC. For this purpose, a capacitor, a diode bridge and an electric resistance were chosen to be mounted on a circuit board.

The diode bridge developed by the author, with silicon terminals, is illustrated in figure 7, consisting of 4 diodes D1 to D4, was chosen based on the work developed by

Marques (2016). This bridge when receiving the sinusoidal signal from the AC generator converts it into a more stable and smoother signal due to the integration of the capacitor in this system.



Figure 7. Rectifier bridge.

### Data Acquisition

To acquire the processed data from the displacement sensor and the load cell, an acquiring device is required to establish a connection between the experimental apparatus and one computer. For this purpose, a NI® USB-6251 data acquisition board was chosen (Figure 8). This DAQ has 24 digital inputs and outputs, 16 analog inputs and 2 analog outputs and it also offers 2 32-bit counters/timers and digital trigger functions.



Figure 8. NI® USB-6251 data acquisition board.

It also has been selected for offering reliable data acquisition functions in a wide range of applications and an acquisition frequency of up to 100,000 points per second. Ultimately it can receive voltage values up to  $\pm 10$  volts and can return up to  $\pm 5$  volts.

### 2.4. Cutting Tool and Fixation Devices

During the present dissertation, only one cutting tool was used, remaining unmodified by the author throughout the tests.

### Cutting Tool

For these tests it was chosen a quadrangular profile cutting tool with tungsten carbide elements shown in figure 9, with tool rake angle and clearance angle of  $7^\circ$  degrees. Since this tool is made of a cemented carbide, a hard metal, it is suitable for cutting materials such as aluminum, also resisting to abrasion and able to withstand high working temperatures, being able to preserve the sharp edge of the cutting tool surface easily than the rest of the materials present in other tools. This tool was constantly polished with polishing abrasive sandpaper of grit 800 and then 1200, in each pass.

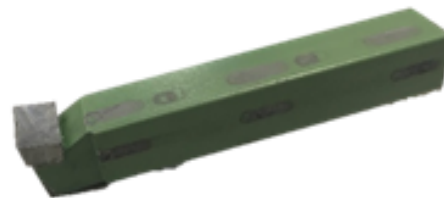


Figure 9. Cutting tool.

### Cutting Tool Fixation Device

The positioning of the tool is a key issue as it will affect how the experiments will proceed. A cutting tool support developed by Kistler® was used for this purpose as shown in figure 10. This device can be easily integrated into the load cell through several matching holes. This support has some components that allow a better adjustment of the tool: a metal plate, an "L" metal bar with a hole to support a micrometer and a set of four metal cubes that allow the "L" bar to be fixed to the fixation device.



Figure 10. Tool fixation device.

## Specimen Fixation Device

The fixation of the specimen into the movable steel guide was designed accordingly the incorporated holes in this guide, not having to machine it, potentially causing some unwanted imperfections, since it must be perfectly guided by the bearing housings. The movable guide has a length of 480 mm and a series of holes. The specimen fixation device developed by the author is shown in figure 11. This holder contains two horizontal screws to ensure the steadiness of the specimen and a vertical screw to avoid slipping due to the bolt load exerted only horizontally.



Figure 11. Specimen fixation device.

It is possible to note that both these fixation devices are adjustable, allowing the specimen to be adjusted to the width of the cutting tool rake face, regardless of its size. The specimen support device is 94 mm long and 32 mm wide.

## 2.5. Experimental Apparatus Installation

Since all the components are defined and manufactured, the experimental apparatus shown in figure 12 was then assembled. The machine tool is based on a structure that is screwed to the ground, further increasing its rigidity and stability. The electromagnetic actuator support is also screwed to the floor in cases of high current induced on metal cutting tests, to avoid misalign with the steel guide. The electromagnetic actuator is controlled by five capacitors that could store electrical current up to 400 Volts, enabling cutting speeds of 200 m/min acquired by Fernandes (2017), a value used by the author in some cutting tests.



Figure 12. Experimental apparatus.

A detailed scheme of this system is displayed in figure 13. Connections represented with a darker tone express the components that are constantly connected to the UPS.

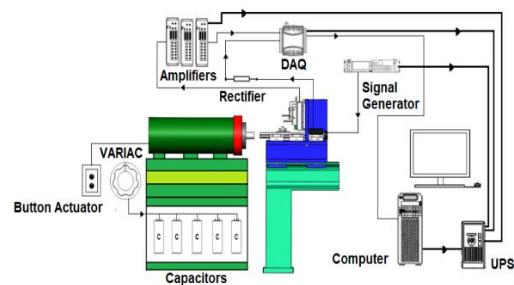


Figure 13. Experimental apparatus connection scheme.

## 3. Materials and Methods

The material used for the cutting tests is an AA1050 aluminum specimen (Figure 14) and is presented as practically pure aluminum (99.5%). This aluminum is widely used in the chemical, pharmaceutical and food industry in, for example, aluminum food containers. It is also used in small components of household utensils, cooling system fins, lithographic plates, lamp reflectors and cable cladding.

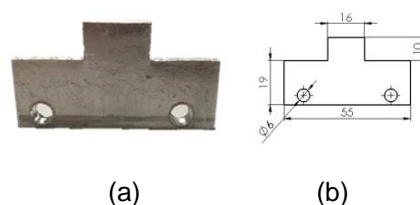


Figure 14. a) Aluminum specimen; b) Specimen dimensions.

For the lubrication experiments, glycerin was used to lubricate the specimen. This choice was taken since glycerin has no additives, being practically pure and has inert properties due to the glycerol, which will prevent chemical reactions. One of the great advantages is that can be applied without a controlled atmosphere, requiring a closed system, because it creates a protective layer applied locally, protecting the surface of the specimen.

A test plan was designed for this test machine to perform. The test plan consists of four test cases, which will be presented in table 1. In a first step, these experiments will be performed without lubricant, for three values of undeformed chip thickness of 0.02, 0.05 and 0.1 mm. Then, glycerin will act as a lubricant in the cutting process, both for quasi-static and high velocity conditions, for the same thicknesses as before.

Table 1. Test plan

Case	Material	$t_0$ (mm)	Velocity Conditions	Lubricant	$\alpha$ (°)	$\sigma$ (°)
1	Aluminum	0,1 0,05 0,02	Quasi-Static	-----	7	7
2	Aluminum	0,1 0,05 0,02	High Velocity	-----	7	7
3	Aluminum	0,1 0,05 0,02	Quasi-Static	Glycerin	7	7
4	Aluminum	0,1 0,05 0,02	High Velocity	Glycerin	7	7

## 4. Results and Discussion

### 4.1. Machine Testing Inspection

An inspection will be done on this test machine regarding the guiding system where the specimen is located, as well as the stiffness of its structure. This test machine does not show any torque or warp influences from misalignment or component offsets. The bearing bearings are aligned with the center of the machine, otherwise there could be no fluency in the passage of the guide through the three bearing housings.

### Guiding System Inspection

For the guiding system inspection, successive calibrated weights of 4.5 kg each were placed until a total of 22.5 kg, using the indicator to measure any gaps or lack of stiffness, as shown in figure 15. During this test, the clock pointer did not move.



Figure 15. Calibrated weights inspection test.

### Structure Inspection

Since the load cell used in these experiments can process loads up to 10000 N, a stiffness study on the critical bolt-member connections was performed up to these maximum applied load values, and it is described in figure 16. It is possible to observe from the graphic that for maximum possible loads involved in the tests, the bolt-member connections will not slide or separate, having elongations in the order of  $1.2 \cdot 10^{-6}$  mm for M8 bolt thread and  $2,3 \cdot 10^{-6}$  mm for M10 bolt thread.

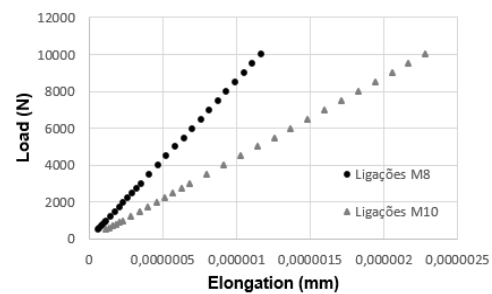


Figure 16. Relation between the applied load and the elongation of the bolt-member connection, for both bolt thread dimensions.

### 4.2. Cutting forces evaluation

#### Quasi-Steady Conditions

The experiments with 0,1 mm of undeformed chip thickness shown in figure 17 exhibit a

zone where cutting and thrust forces stabilize. This stabilization landing is related to the high undeformed chip thickness, approaching a typical orthogonal cutting graph. The quasi-static tests have a cutting speed of 2 m/min.

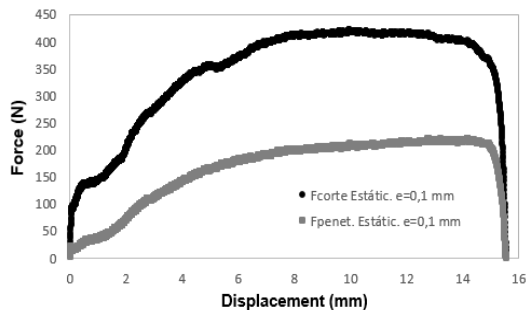


Figure 17. Cutting and thrust forces resulted from a test on an AA1050 aluminum specimen for an undeformed chip thickness of 0.1 mm as function of displacement.

### High Velocity Conditions

For high velocity experiments on aluminum A1050, an oscillation of the cutting forces is present (Figure 18). This characteristic has a certain repeatability throughout the cutting force rather than the trust force. This amplitude decreases when increasing undeformed chip thickness. The high velocity tests have a cutting speed of 670 m/min.

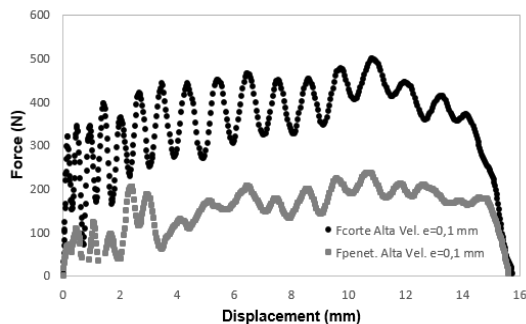


Figure 18. Cutting and thrust forces resulted from a test on an AA1050 aluminum specimen for an undeformed chip thickness of 0.1 mm as function of displacement, in high velocity.

An observation analysis was performed on the specimen's machined surface. It is possible to observe the marks left on the surface after a high velocity test, shown in figure 19.

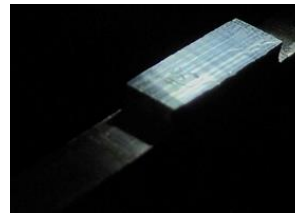


Figure 19. Specimen's surface

To promote a stationary cut, a similar geometric specimen of equal thickness but with 48 mm in length was used. This change did not result in a stability plateau, concluding that oscillations are unavoidable when cutting aluminum AA1050 in high velocity conditions, shown in figure 20.

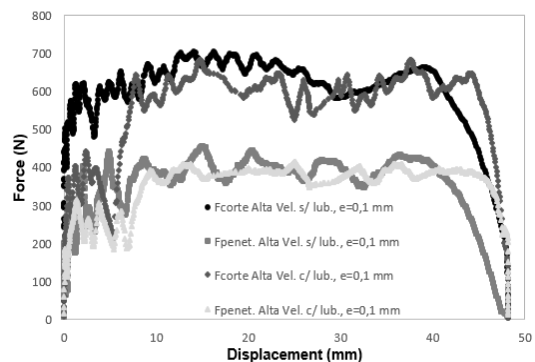


Figure 20. Cutting and thrust forces from a 48 mm long AA150 aluminum specimen cutting test for an undeformed chip thickness of 0.1 mm, as function of displacement, in high speed, with and without lubricant.

### 4.3. Influence of the lubricant evaluation

#### Quasi-Steady Conditions

The cutting forces are reduced with addition of glycerin. In the tests with undeformed chip thicknesses of 0.1 and 0.05 mm, the cutting force decreases with glycerin application at a rate of 3% and 4%, respectively, whereas for the thickness of 0.02 mm there is a general reduction around 20%, as shown in figure 21.

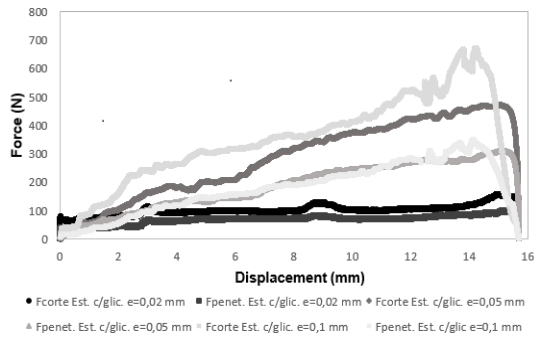


Figure 21. Cutting and thrust forces resulted from a test on an AA1050 aluminum specimen with glycerin as function of displacement, in quasi-state conditions.

### High Velocity Conditions

In figure 22 it should be noted that although the evolution of forces along the displacement is not as standardized as the non-lubricant tests, the cutting force decreases with the addition of glycerin, with a general reduction of 4%.

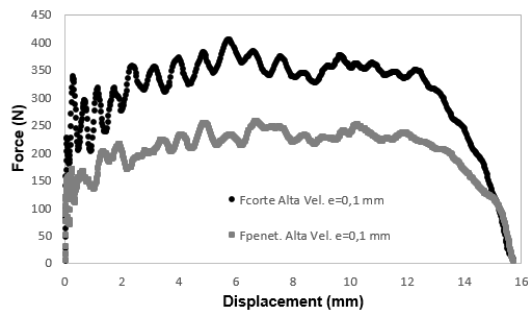


Figure 22. Cutting and thrust forces resulted from a test on an AA1050 aluminum specimen for an undeformed chip thickness of 0.1 mm with glycerin as function of displacement, in high velocity conditions.

### Specific Cutting Pressure

The specific cutting pressure is defined as a force per unit area, used as an efficiency indicator, also referred to as specific cutting power, the power consumed per unit volume of material cut in the time unit. It is possible to observe in figure 23 the typical behavior of this variable that increases with the reduction of the undeformed chip thickness, and its absolute value decreases with the addition of lubricant, either in quasi-static or high velocity conditions.

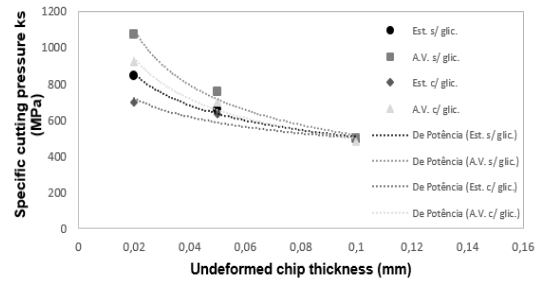


Figure 23. Specific cutting pressure as function of the undeformed chip thickness, for both quasi-static and high velocity conditions, with and without lubricant.

It should be noted that this value is practically the same under any of the conditions for an undeformed chip thickness of 0.1 mm.

### Chip Inspection

The process of obtaining and measuring chips is a time-consuming and careful process, using the microscope to do so. The chip shown in figure 24 is the resultant chip of a high velocity test with an undeformed chip thickness of 0,05 mm, without addition of glycerin. The chip dimensioning is carried out in three phases of their total length, obtaining the average chip thickness.

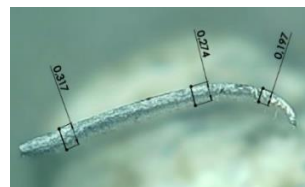


Figure 24. Chip dimensioning.

### Chip Compression Ratio

For a better understanding of the chips resulted from the cutting experiments, a study of the chip compression ratio was carried out. If there is a high chip compression ratio for a given material to be tested, it means that the degree of plastic deformation of that material will be elevated. The action of the chip compression ratio occurs when the chip slides through the tool's rake face, being countered by the friction. The chip the goes undergoes a plastic deformation, increasing its thickness. When analyzing figure 25 we can observe



that chip compression ratio is higher in the quasi-static conditions and lower in high velocity conditions, reducing with the increase of the undeformed chip thickness.

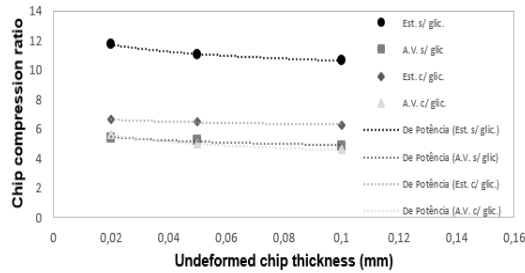


Figure 25. Chip compression ratio of aluminum AA1050 as a function of the undeformed chip thickness, for both velocity conditions, with and without lubrication.

In quasi-static conditions experiments without glycerin the results of the chip compression ratio are around the value of 11, a very high value due to the high compression of the chip when being removed. For the remaining cases the values of the chip compression ratio are between 4.5 and 6.5, slightly high values in the orthogonal cutting analysis. However, in the work developed by Cordeiro (2010), testing aluminum AA1050 specimens resulted in a chip compression ratio around 7, for a specimen with 200 mm width in quasi-static conditions.

### Shear Plane Angle

Figure 26 shows the shear plane angle. When the cutting force is reduced, the shear plane angle increases, so when adding lubricant to the process the cutting angle theoretically should increase, as it can be seen in figure 26, showing that for high velocity condition tests, the addition of a glycerin will not significantly alter this value, remaining at an average shear plane angle of 11°. For the quasi-static tests, the addition of glycerin will increase this value from 5° to 9°.

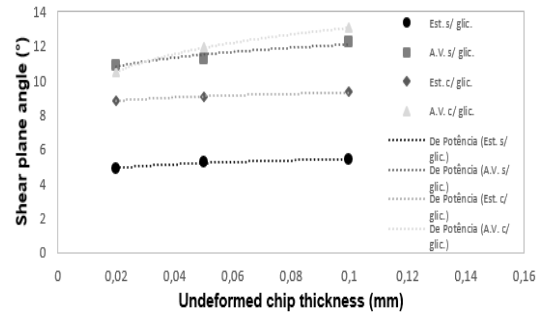


Figure 26. Shear plane angle of aluminum AA1050 as a function of the undeformed chip thickness, for both velocity conditions, with and without lubrication.

### Friction Coefficient

Figure 27 shows the evolution of the friction coefficient (obtained through the Coloumb model). The results obtained in this aluminum AA1050 experiments show that the friction coefficient tends to decrease when increasing the undeformed chip thickness, regardless the addition of lubricant or velocity condition. These results also show that with the addition of glycerin, the friction coefficient increases, not being an expected result in a first observation.

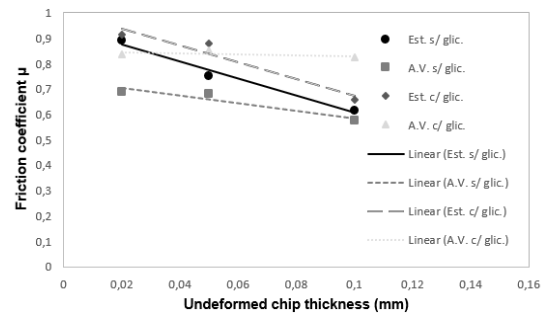


Figure 27. Friction coefficient of aluminum AA1050 as a function of the undeformed chip thickness, for both velocity conditions, with and without lubrication.

It is possible to observe in figure 27 that the friction coefficient in quasi-static conditions increases on average by 9% with the addition of glycerin, while in high velocity conditions it increases on average by 30%. This is due to the fact that by adding glycerin, the chip has a better outflow, reducing the area of contact on the tool's rake face, promoting a better flow in this surface. However, there was no reduction of the contact at the tool's clearance face.

---

## 5. Conclusions

In the first phase of conceptualization of this testing machine it was designed to guarantee a high stiffness in order to support external load applied without its yield or vibration, always focusing on the parallelism and orthogonality among the several constituent components, trying to suppress the existence of gaps, misalignments or warps. A study was made on the bolt-member connections of the testing machine, showing that it can withstand elevated external loads.

The successive tests carried throughout this dissertation indicate that the experiments are more comparable when performed from a greater undeformed chip thickness to a smaller one, since there is more homogeneity of material the larger the cutting depth reached.

The cutting process of AA1050 aluminum in high velocity conditions only exhibits minimally stable cutting forces evolutions when undeformed chip thickness reaches the value of 0.1 mm, still exhibiting small-amplitude oscillations. In an attempt to stabilize the cutting forces, a 48 mm long AA1050 aluminum specimen was tested, showing again small oscillations of cutting forces along its surface without ever reaching a stationarity *plateau*, concluding that it is an intrinsic characteristic of this material.

The use of glycerin as a lubricant in this process resulted in an increase in the friction coefficient in the order of 9% and 30% for quasi-static and high velocity conditions, respectively, due to the increase ratio in thrust forces being greater than the decreasing ratio of the cutting forces. This was also demonstrated by other tests in this test machine which demonstrated for the same material, with a different lubricant, the friction coefficient increases by 10% for high velocity conditions (Campos J., Coelho J., 2019).

## 6. References

- Campos J., Coelho J., Private communication, IST, Lisboa, 2019
- Cordeiro D., *Avaliação Numérica e Experimental de Tensões Residuais*, IST, Lisbon, 2010.
- Fernandes J., *A importância do oxigénio no comportamento tribológico do corte por arranque de aparas*, IST, Lisbon, 2017.
- Lee E. H., Shaffer B.W., *Theory of plasticity applied to a problem of machining*, J. appl. Mech., Trans. ASME, vol. 73, 405-413, 1951.
- Marques O., *Estudo dos efeitos de escala na resistência mecânica das ligas AA1050 e AA1085*, IST, Lisbon, 2016.
- Merchant M.E., J. Applied Physics., vol. 66, 168-170, 1944.
- Myers D., *Surfaces, Interfaces, and Colloids, Principles and Applications*, Wiley Global Education, New York, 1999.
- Noble D., *Forces of Production: A Social History of Industrial Automation*, Transaction Publishers, 2011.
- Rolt L. T. C., *Tools for the Job*, Batsford, London, U.K., 1965; Reissued by HSMO Press, London, 1986.
- Woodbury R. S., *History of the Lathe*, Society for the History of Technology, Cleveland, OH, 1961.